Proceedings of ASME FEDSM'02
ASME 2002 Fluids Engineering Division Summer Meeting
Montreal, Quebec, Canada, July 14-18, 2002

FEDSM2002-31289

EFFECTS OF APPLYING A STOCHASTIC REBOUND MODEL IN EROSION PREDICTION OF ELBOW AND PLUGGED TEE

Xianghui Chen, Brenton S. McLaury, and Siamack A. Shirazi
Erosion/Corrosion Research Center
Mechanical Engineering Department
The University of Tulsa
Tulsa, OK 74104
E-mail: xianghui-chen@utulsa.edu, brenton-mclaury@utulsa.edu, siamack-shirazi@utulsa.edu

ABSTRACT

Solid particle erosion is a complex phenomenon that depends on many factors such as particle and fluid characteristics, type of material being eroded, and flow geometry. Fittings used in the oil and gas industry such as elbows are susceptible to erosion when solid particles are present in the flow. The momentum of particles carries them across streamlines and the particles impinge the outer wall of the elbow resulting in erosion damage. In an erosive environment, plugged tees are commonly used instead of elbows to reduce the erosion especially where space considerations are important and long-radius elbows can not be used. However, it is unclear how much of a reduction in erosion occurs by replacing an elbow with a plugged tee.

In order to compare the erosion in an elbow and a plugged tee exposed to the same flow conditions, a CFD-based erosion prediction model is applied. The model has three primary steps: flow modeling, particle tracking, and applying erosion equations. The results from the model agree with experimental findings for the elbow geometry. However, the simulation results for erosion rate generated for the plugged tee requires a stochastic approach. Results obtained with the erosion prediction model before and after this modification are shown.

Keywords: CFD, Stochastic Rebound Model, Erosion Prediction, Elbow, Plugged Tee.

NOMENCLATURE

BH	Brinell hardness of wall material
C_D	drag force coefficient
D	pipe inner diameter
d_p	particle diameter
e_{par}	coefficient of restitution of the parallel velocity component
e_{per}	coefficient of restitution of perpendicular velocity component
F_A	added mass force
F_B	buoyancy force
F_D	drag force
F_P	pressure gradient force
F_S	particle shape coefficient
g	gravitational acceleration
k	turbulent kinetic energy
L	plugged section length (L/D=1)
m_p	mass of particle
P	pressure
r	radius of curvature of of the standard elbow (r/D=1.5)
Re_S	particle relative Reynolds number
u'	velocity fluctuation of carrier fluid
V	particle impingement velocity
V_f	fluid velocity
V_p	particle velocity
Δm_i	wall mass loss caused by each particle impingement
θ	particle impact angle
μ	fluid viscosity
ρ_f	fluid density
ρ_p	particle density
σ_{par}	standard deviation of the coefficient e_{par}
σ_{per}	standard deviation of the coefficient e_{per}

INTRODUCTION

Fluid flows laden with particles are commonly found in many engineering industries such as the oil and gas industry. During the production of oil and gas, sand particles entrained in the production fluid are transported with the carrier fluid via piping systems. The sand degrades the inside surfaces of pipes, valves, fittings, and other equipment, resulting in erosion damage to the equipment. Erosion can be dangerous and expensive. High erosion rates can lead to frequent replacement of the damaged equipment. Severe erosion problems can even cause failures of the piping system. In addition, component failure can result in expensive system shutdowns, resulting in loss of valuable production revenue.

The erosion phenomenon is highly complicated and a wide range of parameters effect the erosion severity, such as production flow rate, sand rate, fluid properties, sand properties, sand shape and size, wall material of equipment, and geometry of the equipment. Complex geometries are found in piping systems and equipment used by the oil and gas industry. Since these geometries often change the direction of the flow, particles that are entrained in the fluid can cross streamlines and impinge the wall, causing erosion to occur. This erosion can eventually result in failure of the geometry in service. The ability to predict erosion rates not only allows one to estimate service life, but also enables the detection of locations in the geometry where severe erosion is likely to occur.

An elbow is a common geometry used in piping systems to redirect flow. Elbows alter the fluid velocity profiles from straight pipe flow behavior. Particles that are entrained in the flow tend to follow the fluid streamlines. However, the particles can acquire sufficient momentum to deviate the flow streamlines and impinge the wall. Therefore, elbows are especially vulnerable to erosive wear due to solid particle impingement under certain flow conditions. Because elbows are vulnerable to solid particle erosion failure, plugged tees are commonly used instead of elbows if severe erosion is anticipated. However, a plugged tee also redirects the flow and has streamlines that change very rapidly. Due to the change in flow direction, sand impingement on the walls is inevitable which will result in erosion damage to plugged tees. At this time, the reduction in erosion rate by replacing an elbow with a plugged tee is not known or if the plugged tee is even beneficial for all cases.

The Erosion/Corrosion Research Center (E/CRC) at The University of Tulsa has developed a procedure for generating erosion predictions. The procedure utilizes a commercially available computational fluid dynamics (CFD) code. A comprehensive erosion prediction procedure that involves flow modeling, particle tracking, and erosion equations has been implemented into the commercial code by Edwards [1]. As a result, an erosion prediction technique that is applicable to a wide range of complex three-dimensional geometries has been developed. The erosion prediction procedure has been verified for elbow cases with some experimental data and showed good agreement [2].

Description of Computational Model

The erosion prediction procedure was added to a commercially available CFD code, CFX, which was developed by AEA Technology [3]. This code uses a finite difference approach to solve the Navier-Stokes equations. CFX requires the user to specify the flow conditions such as fluid properties, and flow rates (or inlet velocities) as well as the geometry.

Within CFX, there are several turbulence models available. In this research, the differential stress turbulence model is used. The flow simulation contains all the information such as velocity components, turbulence quantities (turbulent kinetic energy and dissipation rate) that are used in the prediction of particle trajectories.

Using information generated by the flow simulation, particle tracking and erosion calculations are then performed. A large number of particles are introduced at the inlet of the geometry to obtain the particle trajectories. A large number of particles, on the order of many thousand, are normally required to obtain a reasonable statistical distribution and to reduce scatter in the erosion predictions. Each particle is tracked separately through the flow field and particle impingement information such as speed, angle, and location is collected as a particle strikes the wall. This information is then used by a set of empirical erosion equations to predict penetration rate. These equations account for the impingement speed and angle, as well as the particle shape and mechanical properties of the wall material.

In numerical simulations of turbulent particulate two-phase flows, the Lagrangian approach is used for the particle phase. The particle equation of motion used in the code is given as [4]:

$$m_p \frac{dV_p}{dt} = F_D + F_P + F_B + F_A \tag{1}$$

The above equation consists of

- Drag force:

$$F_D = C_D \rho_f \frac{\pi d_p{}^2}{8} \left| V_p - V_f \right| \left(V_p - V_f \right) \tag{2}$$

where C_D is the drag force coefficient, defined as

$$C_D = \frac{24}{Re_S}\left(1 + 0.15 Re_S{}^{0.687}\right) \tag{3}$$

where Re_S is the particle relative Reynolds number, defined by

$$Re_S = \frac{\rho_f \left(V_p - V_f\right) d_p}{\mu} \tag{4}$$

- Pressure gradient force:

$$F_P = \frac{1}{4} \pi d_p{}^3 \nabla P \tag{5}$$

- Buoyancy force:

$$F_B = \frac{1}{6} \pi d_p{}^3 \left(\rho_p - \rho_f\right) g \tag{6}$$

- Added mass force:

$$F_A = -\frac{1}{12} \pi d_p{}^3 \rho_p \frac{dV_p}{dt} \tag{7}$$

The effect of the turbulence on the particle motion is included using the study of Gosman and Ioannides [5]. This model takes into account the crossing trajectories and eddy lifetime to calculate the interaction time of particle and the eddy. In this approach, the turbulence is assumed to be isotropic and to possess a Gaussian probability distribution in the fluctuating velocity. The mean of the fluctuating velocities is zero and the standard deviation, u', is given by the predicted turbulent kinetic energy field:

$$u' = \sqrt{(2k/3)} \tag{8}$$

The erosion model used by Edwards [1] is applied in this research. Impingement information, such as impact speed and impact angle, is gathered as particles hit the wall of the geometry. Using this information the erosion ratio can be calculated. The erosion ratio is defined as the mass loss of the pipe wall due to erosion divided by the mass of particle impacting the wall. The erosion ratio depends on the particle impact speed and impact angle. The erosion ratio is given by

$$ER = \frac{\Delta m_i}{m_p} = A\ F_s\ V^n\ f(\theta) \tag{9}$$

where ER is the erosion ratio (kg/kg); A is an empirical constant; V is the particle impingement speed, and F_s is a particle shape coefficient; F_s = 1.0 for sharp (angular), 0.53 for semi-rounded, or 0.2 for fully rounded sand particles. While f(θ) is the function of the impact angle that is given by

$$f(\theta) = \begin{cases} a\theta^2 + b\theta & \text{for}\ \theta \le \varphi \\ x\cos^2\theta \sin(w\theta) + y\sin^2\theta + z & \text{for}\ \theta > \varphi \end{cases} \tag{10}$$

where φ a, b, w, x, y, and z are empirical constants that depend on the material being eroded. The suitable values of the model constants, assuming V has units of ft/s, are provided in Table 1 for carbon steel [1].

In order to accurately predict the particle trajectories an appropriate rebound model describing the particle-wall collision must be used. At impact, the reflected velocity of the particle is lower than the incoming velocity due to energy transfer. This impact signature is described by the momentum-based coefficient of restitution, e. The CFD code originally assumes that the impact signature can be adequately described through consideration of the normal velocity component alone and that the coefficient is angle insensitive. However, Grant and Tabakoff [6] and Forder [7] have shown that the coefficient is reduced at impact. Forder [7] proposed the following coefficient relationships for perpendicular and parallel velocity components for AISI 4130:

$$e_{per} = 0.988 - 0.78\theta + 0.19\theta^2 - 0.024\theta^3 + 0.0027\theta^4 \tag{11}$$

$$e_{par} = 1 - 0.78\theta + 0.84\theta^2 - 0.21\theta^3 + 0.028\theta^4 - 0.022\theta^5 \tag{12}$$

Table 1. Empirical Constants Used in the Erosion Model.

Material	Carbon Steel
A	1559 $BH^{-0.59}$ x 10^{-8}
Φ	15 º
a	-38.4
b	22.7
x	0.3147
w	1
y	0.03609
z	0.2532
n	1.73

Grant and Tabakoff [6] and Sommerfeld [8,9] treated the rebound dynamics of the particles in a statistical sense. Based on experimental data (for 2024 Aluminum and 200 µm sand particles), Grant and Tabakoff postulated the mean values of the coefficients of restitution (e_{per} and e_{par}), which are incoming angle-dependent distributions with angle-dependent standard deviations (σ_{per} and σ_{par}).

$$e_{per} = 0.993 - 1.76\theta + 1.56\theta^2 - 0.49\theta^3 \tag{13}$$

$$e_{par} = 0.998 - 1.66\theta + 2.11\theta^2 - 0.67\theta^3 \tag{14}$$

$$\sigma_{per} = -0.0005 + 0.62\theta - 0.535\theta^2 + 0.089\theta^3 \tag{15}$$

$$\sigma_{par} = 2.15\theta - 5.02\theta^2 + 4.05\theta^3 - 1.085\theta^4 \tag{16}$$

Results and Discussion

In order to study the relative amount of erosion occurring between an elbow and a plugged tee (as seen in Figure 1), erosion simulations were planned for each geometry operating under two conditions. The first condition used water as the carrier fluid, and the second condition used air as the carrier fluid. For the water cases, 100,000 particle trajectories were simulated, and 10,000 particle trajectories were determined for the air cases. These numbers of particles provided erosion results that were independent of number of particles used in the simulations. Many parameters for the simulations were the same for both carrier fluids. Table 2 contains the parameters defining sand rate and size as well as geometry diameter and material. For the first round of simulations, the Forder rebound model was used for particle-wall collisions.

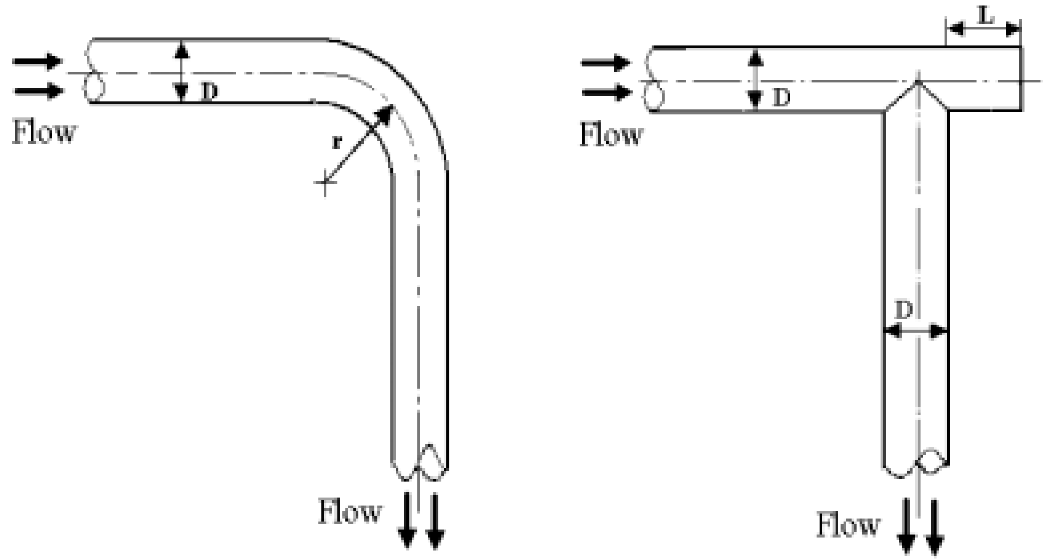

Figure 1. Geometry of the Standard Elbow and Plugged Tee.

Table 2. Simulated Cases

Carrier Fluid	Water	Air
Fluid Velocity	20 ft/s	100 ft/s
Pipe Diameter	2”	
Sand Flowrate	10 lb/day	
Sand Diameter	50 µm	
Wall Material	Carbon Steel, BH=120	

The first simulation used water as the carrier fluid with an inlet velocity of 20 ft/s through an elbow. Figure 2 is a surface plot of the erosion rate on the elbow for this case. This figure shows that the maximum erosion occurs near the exit of the elbow with a maximum erosion rate of 0.055 mpy. The next simulation also used water as the carrier fluid with an inlet velocity of 20 ft/s, but the geometry was a plugged tee. Figure 3 is a surface plot of the erosion rate on the plugged tee for this case. This figure shows that the maximum erosion occurs at the intersection of the plugged section and the downstream section. The erosion rate at this location is 0.58 mpy, an order of magnitude greater than the erosion in the elbow. This result is not surprising since the number of impacts is greater for the plugged tee. The elbow redirects the flow more gradually than the plugged tee, so the particles are able to follow the streamlines more closely in the elbow than in the plugged tee.

The next set of simulations used air as the carrier fluid with an inlet velocity of 100 ft/s. Figure 4 shows the erosion rate for the elbow geometry exposed to these conditions. This figure shows that the area of maximum erosion moved farther upstream for the air case than in the water case for the elbow. Air is less dense than water causing the transfer of momentum between the fluid and the particles to be less efficient; therefore, particles impinge more rapidly for the air case. The maximum erosion rate in Figure 4 is 4,320 mpy. Figure 5 shows the erosion rate for the plugged tee using air as the carrier fluid. The maximum erosion rate in Figure 5 is 61,500 mpy and this occurs in a small concentrated area in the plugged section. It was anticipated that the maximum erosion would occur on the plug perpendicular to the inlet flow direction. Since, this did not occur the particle motion was investigated. Figure 6 shows the deposition rate of the particles in mass of particles impinged per unit area. The areas with high deposition rates correspond to predicted locations of high erosion rate. Ten representative particle trajectories are shown in Figure 7. This figure demonstrates that the particles become trapped in the plugged section of the tee. Some individual particles impinge the wall in this section hundreds of times along a recirculation path. The particles repeat the same path many times rebounding in nearly an identical manner. This is not physical because of the stochastic nature of the particle-wall collision rebound process.

In order to represent the rebound as a stochastic event, the rebound model proposed by Grant and Tabakoff in Equations (13) to (16) was applied. The coefficient of restitution applied was determined from a random sampling of a Gaussian distribution with the mean provided by Equations (13) and (14) and standard deviations provided by Equations (15) and (16). The simulations for the water and air cases were performed again with the revised rebound model.

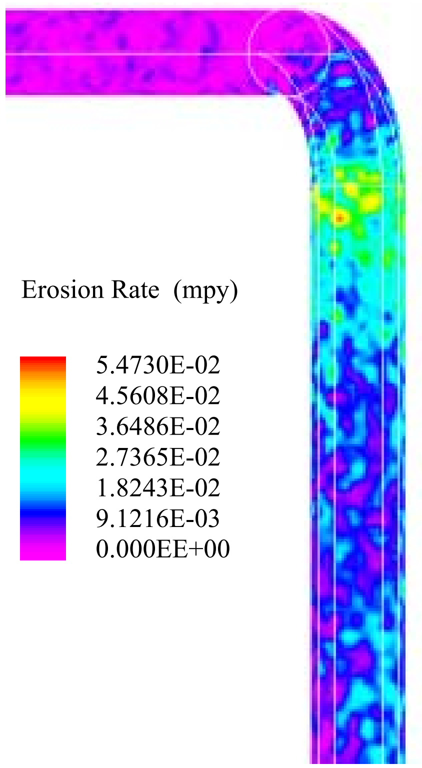

Figure 2. Erosion of the Elbow for the Water Case Based on Forder Rebound Model.

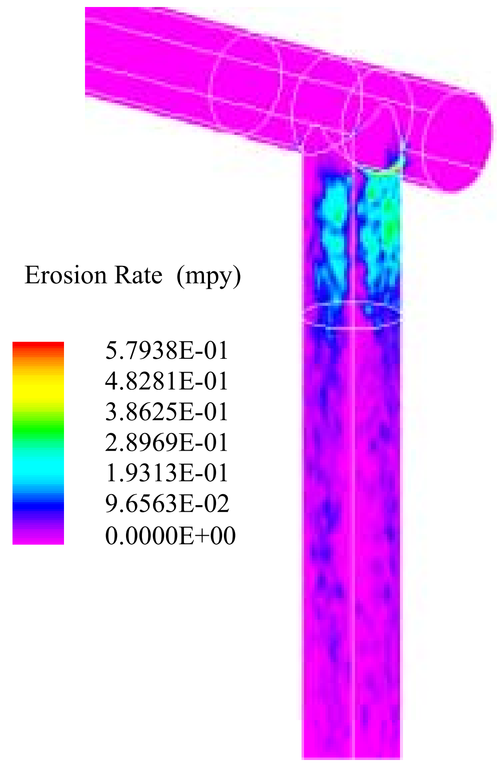

Figure 3. Erosion of the Plugged Tee for the Water Case Based on Forder Rebound Model.

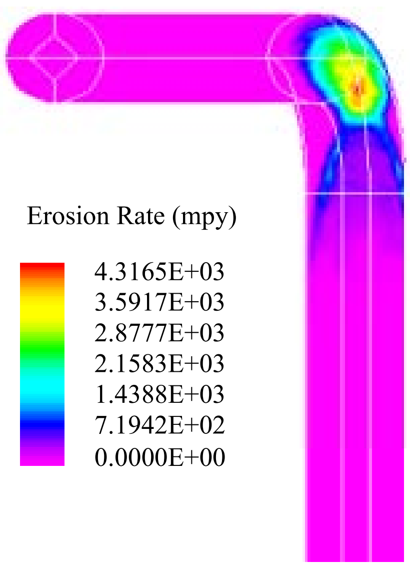

Figure 4. Erosion of the Elbow for the Air Case Based on Forder Rebound Model.

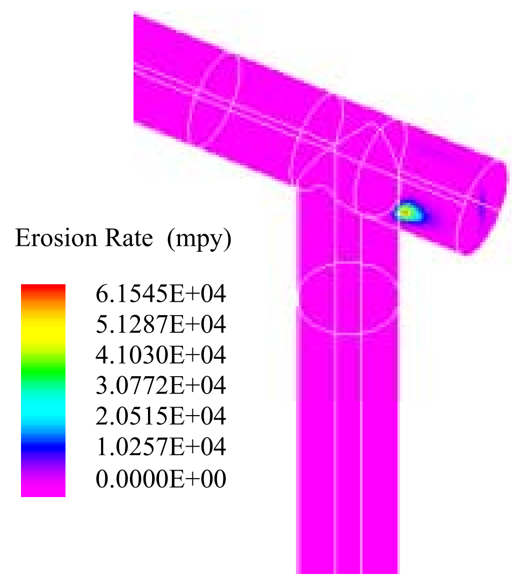

Figure 5. Erosion of the Plugged Tee for the Air Case Based on Forder Rebound Model.

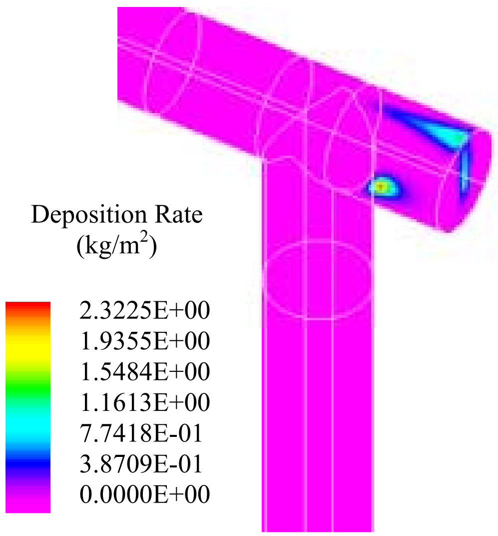

Figure 6. Deposition Rate of Sand Particles in Plugged Tee for the Air Case Based on Forder Rebound Model.

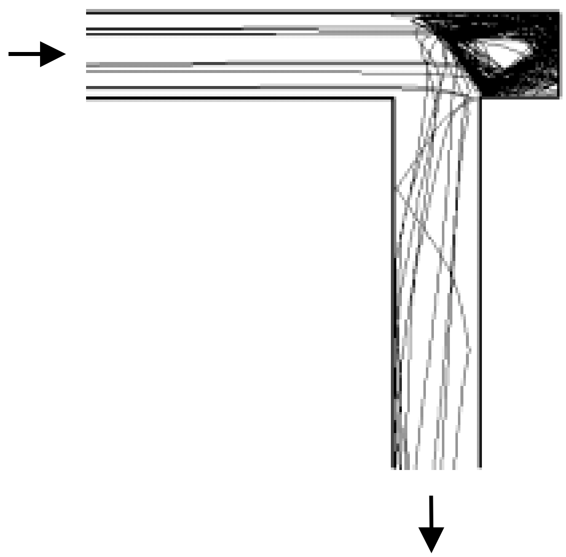

Figure 7. Sample Particle Trajectories in the Plugged Tee for the Air Case Based on the Forder Rebound Model.

Figures 8 and 9 show the erosion rates for the water case in the elbow and plugged tee, respectively. These results are very similar to the results obtained with the previous rebound model shown in Figures 2 and 3. However, differences in erosion rates are apparent for the air cases using the different rebound model approaches. Figure 10 shows the erosion rate in the elbow for the air case using the stochastic rebound model. The location of maximum erosion is approximately the same as that in Figure 4, but the erosion rate has increased slightly. Figure 11 shows the erosion rate for the plugged tee using the stochastic rebound model. These results seem more physical than the previous results for the plugged tee air case. The maximum erosion rate occurs on the back of the plugged section and the erosion rate has dropped below the erosion rate determined in the elbow for the same conditions. To compare the particle motion in the plugged section for both rebound models, the deposition rate and sample particle trajectories are shown in Figures 12 and 13 using the stochastic rebound model. The stochastic rebound model allows the particles to leave the recirculatory path more easily in the plugged section and travel downstream.

Conclusion

A CFD-based erosion prediction procedure developed by E/CRC was used to determine the erosion resulting in elbows and plugged tees. The erosion in each geometry was determined for two cases: air as carrier fluid and water as carrier fluid. The initial simulations applied a rebound model that was not stochastic. When the relatively small particles were traveling in the plugged tee for the air case, they would become trapped in a recirculation zone in the plugged section. A single particle could impinge the plugged section hundreds of times resulting in unrealistic deposition and erosion rates. In order, to predict more physical results a stochastic rebound model using results obtained by Grant and Tabakoff was applied. The results obtained with the stochastic rebound model were similar in the elbow for both the water and air cases and similar in the plugged tee for the water case. However, significant differences occurred in the plugged tee for the air case. More realistic deposition and erosion rates were obtained for this case by applying the stochastic rebound model. The next phase of this study is to obtain experimental erosion data to validate the claims that the updated results are more realistic. The current work demonstrates that a stochastic rebound model is necessary when the geometry contains recirculation zones. This work also demonstrates that it is not always beneficial to use a plugged tee instead of an elbow in an effort to reduce erosion.

ACKNOWLEDGMENTS

The authors would like to acknowledge the member companies of E/CRC for sponsoring this work.

REFERENCES

[1] Edwards, J. K., "Development, Validation, and Application of A Three-Dimensional, CFD-Based Erosion Prediction Procedure," PhD Dissertation, The University of Tulsa, 2000.
[2] Edwards, J.K., McLaury, B.S., and Shirazi, S.A., "Evaluation of Alternative Pipe Bend Fittings in Erosive Service," Paper No. FEDSM00-11245, ASME Fluids Engineering Division Meeting, Boston, MA, June 11-15, 2000.
[3] CFX, "CFX-4.2: Solver," AEA Technology, Oxfordshire, United Kingdom, 1997.
[4] Clift, R., Grace, J.R., and Weber, M.E., Bubbles, Drops, and Particles, USA, 1978.

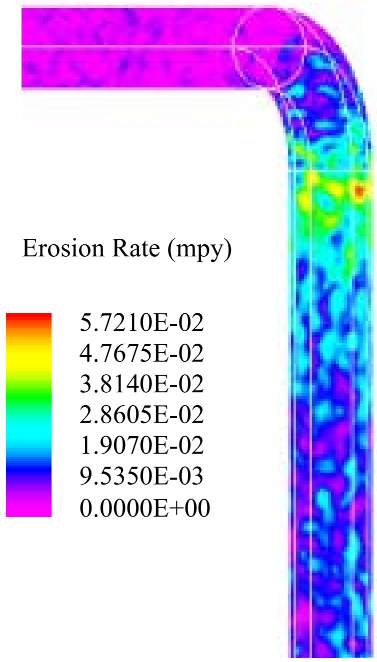

Figure 8. Erosion of the Elbow for the Water Case Based on Grant and Tabakoff Rebound Model.

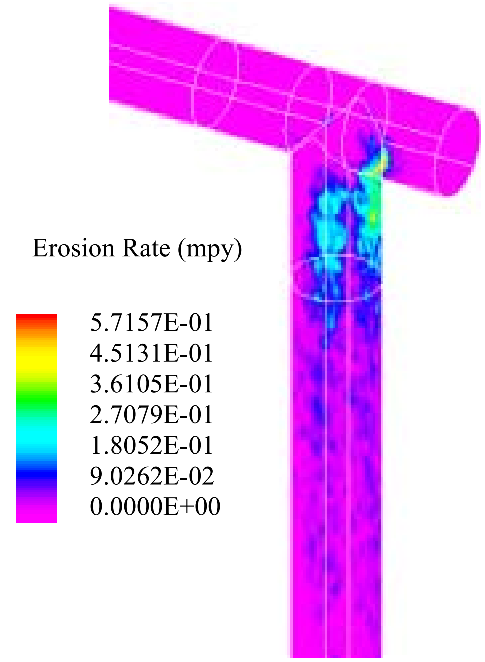

Figure 9. Erosion of the Plugged Tee for the Water Case Based on Grant and Tabakoff Rebound Model.

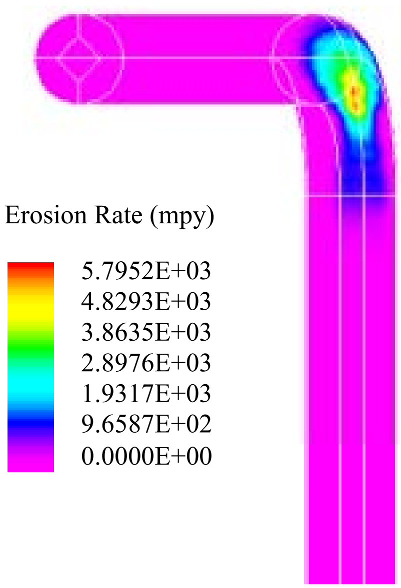

Figure 10. Erosion of the Elbow for the Air Case Based on Grant and Tabakoff Rebound Model.

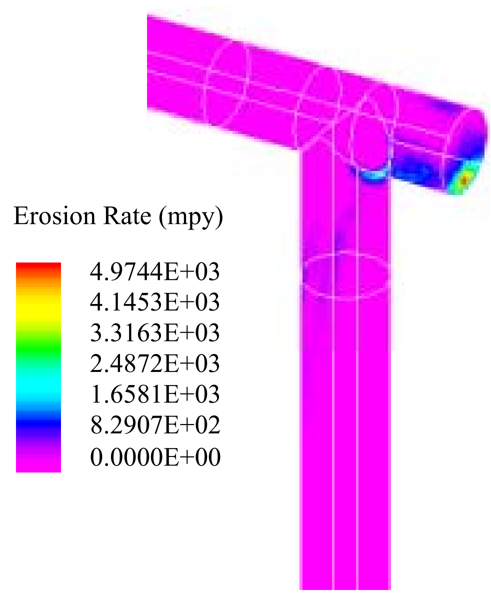

Figure 11. Erosion of the Plugged Tee for the Air Case Based on Grant and Tabakoff Rebound Model.

[5] Gosman, A.D. and Ioannides, E., "Aspects of Computer Simulation of Liquid-Fueled Combustors," Journal of Energy Vol. 7, No. 6, pp. 482-490, 1983.
[6] Grant, T, and Tabakoff, W., "Erosion Prediction in Turbomachinery Resulting From Environmental Solid Particles," Journal of Aircraft 12, pp. 471-47, 1975.
[7] Forder, A., Thew, M., and Harrison, D., "A Numerical Investigation of Solid Particle Erosion Experienced Within Oilfield Control Valves," Wear 216, pp. 184-193, 1998.
[8] Sommerfeld, M " Modeling of Particle-Wall Collisions In Confined Gas-Particle Flows," International Journal Multiphase Flow, Vol. 18, pp. 905-926, 1992.
[9] Sommerfeld, M., "Particle-Wall Collisions: Experimental Studies and Numerical Models," ASME FED-Vol. 166, pp. 183-191, 1993.

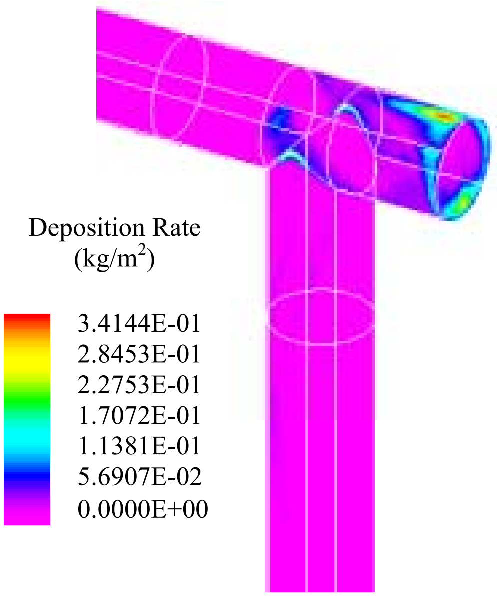

Figure 12. Deposition Rate of Sand Particles in the Plugged Tee for the Air Case Based on Grant and Tabakoff Rebound Model.

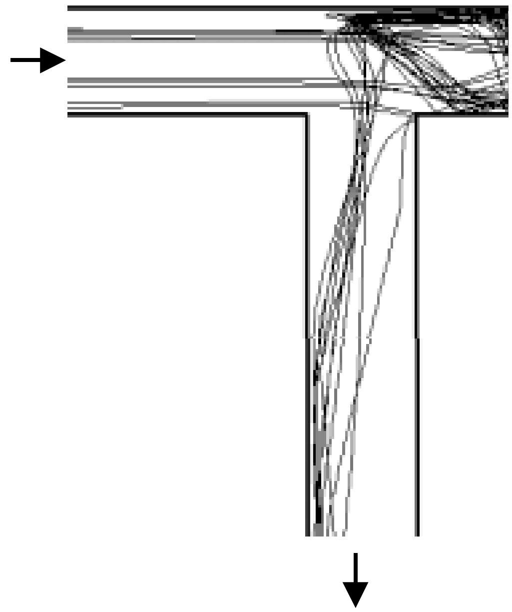

Figure 13. Sample Particle Trajectories in the Plugged Tee for the Air Case Based on the Grant and Tabakoff Rebound Model.

